Nuclear Engineering and Design 441 (2025) 114135

Contents lists available at ScienceDirect

Nuclear Engineering and Design

journal homepage: www.elsevier.com/locate/nucengdes

Uncertainty quantification application on the Phebus FPT1 using the coupling of MELCOR and DAKOTA in a Python environment/architecture

Giuseppe Agnello [a,b,*], Mattia Massone [b], Fulvio Mascari [b,*]

[a] Department of Engineering, University of Palermo, Viale delle Scienze, Ed. 6, 90128 Palermo, Italy
[b] ENEA, C.R. Bologna, Bologna, Italy

ARTICLE INFO

Keywords:
MUSA
Severe Accident
MELCOR
DAKOTA
Uncertainty

ABSTRACT

During the last few years, the international nuclear scientific community involved in the development of deterministic safety analyses in the Severe Accident (SA) domain has focused its interest on the analysis of methodologies for the uncertainty quantification using the state-of-art integral SA codes (e.g. ASTEC, MAAP, MELCOR, etc.). Within this framework, the H2020 "Management and Uncertainty of Severe Accidents" (MUSA) project, coordinated by CIEMAT (Spain), aimed to establish a harmonized approach for the application of uncertainty quantification methodologies to SAs. Along with the MUSA Working Package named "Application of UQ Methods against Integral Experiments", coordinated by ENEA (Italy), the uncertainty analysis methodology has been applied to the Phebus FPT1 experiment. To develop the reference base case, the integral code MELCOR 2.2 has been selected, and it has been coupled with the uncertainty tool DAKOTA to develop the uncertainty analysis. The study has been focused on the degradation and beginning of the aerosol phase of the test, considering the MELCOR aerosol miscellaneous constants as uncertain input parameters and the maximum value of the total mass of aerosol in suspension in the containment atmosphere as Figure of Merit (FOM). The uncertainty analysis permitted a first estimation of the uncertainty bandwidth of the FOM, comparing it with the experimental and reference case values. Among the uncertain input parameters, the dynamic shape factor and the agglomeration shape factor present, respectively, a moderate and significant statistical correlation with the FOM.

1. Introduction

The development of deterministic safety analyses of postulated Severe Accident (SA) sequences has drawn the interest of the international nuclear scientific community. In this regard, the estimation of the Source Term (ST) and the development of SA mitigation strategies heavily rely on these types of studies. Then, integral SA codes have been developed and are continuously updated to simulate the plethora of multi-physics phenomena and processes that characterize a nuclear power plant during a postulated SA, occurring in the reactor cavity, the containment and the Reactor Pressure Vessel (RPV). Examples of these codes are ASTEC (Chatelard et al., 2016), MAAP (EPRI, 2016) and MELCOR (Humphries et al., 2023a,b).

To establish a useful "assessment database" (Mascari et al., 2015), several experimental campaigns have been carried out in the SA domain (NEA/CSNI, 2001; NEA/CSNI, 2024; OECD/NEA/CSNI, 1992; OECD/

Abbreviations: ASTEC, Accident Source Term Evaluation Code; AUQMIE, Application of UQ Methods against Integral Experiments; BEMUSE, Best Estimate Methods Plus Uncertainty and Sensitivity Evaluation; CAV, MELCOR CAV package; CDF, Cumulative Distribution Function; CVH, MELCOR CVH package; CIEMAT, Centro de Investigaciones Energéticas, Medioambientales y Tecnológicas; COR, MELCOR COR package; CV, Control Volume; DAKOTA, Design Analysis Kit for Optimization and Terascale Application; ENEA, Agenzia nazionale per le nuove tecnologie, l'energia e lo sviluppo economico sostenibile; FL, MELCOR FL package; FOM, Figure Of Merit; FP, Fission Product; GUI, Graphic User Interface; HS, MELCOR HS package; IRSN, Institute de Radioprotection et de Sûreté Nucléaire; LP, Lower Plenum; MAAP, Modular Accident Analysis Program; MUSA, Management and Uncertainty of Severe Accidents; PDF, Probability Density Function; PhW, Phenomenological Window; PREMIUM, Post-BEMUSE Reflood Model input Uncertainty Methods; PWR, Pressurized Water Reactor; RN, MELCOR RN package; RPV, Reactor Pressure Vessel; SA, Severe Accident; SG, Steam Generator; SNAP, Symbolic Nuclear Analysis Package; SNL, Sandia National Laboratories; SOARCA, State-Of-the-Art Reactor Consequence Analyses; ST, Source Term; USNRC, United States Nuclear Regulatory Commission; UT, Uncertainty Tool; WP, Working Package.

* Corresponding authors at: Department of Engineering, University of Palermo, Viale delle Scienze, Ed. 6, 90128 Palermo, Italy (G. Agnello); ENEA, C.R. Bologna, Bologna, Italy (Fulvio Mascari).

E-mail addresses: giuseppe.agnello04@unipa.it (G. Agnello), fulvio.mascari@enea.it (F. Mascari).

https://doi.org/10.1016/j.nucengdes.2025.114135
Received 20 January 2025; Received in revised form 18 April 2025; Accepted 5 May 2025
Available online 22 May 2025

NEA/CSNI, 1996; OECD/NEA/CSNI, 2009). However, the state-of-the-art underlines the need to identify, characterize, contextualize and reduce the source of uncertainties that still persist in the SA modelling (Mascari et al., 2019; Mascari et al., 2019; Van Dorsselaere et al., 2016) mostly related to different models (e.g. core degradation models) influencing SA integral code calculations. Consequently, it presupposes a focus on what are the typical phenomena and processes that have not been experimentally studied adopting prototypical geometries and prototype materials (Van Dorsselaere et al., 2016).

Integral SA codes have reached a high level of maturity and have a key role in the development of guidelines for SA management. Considering the complexity of the several phenomena occurring during a SA and the inherent nature of computational codes, the estimation of the uncertainty of code results is currently a central topic in nuclear safety. In this regard, several efforts have been conducted by USNRC in the framework of the SOARCA project which aims to evaluate realistic outcomes in terms of ST evaluation during SAs due to postulated scenarios (Bixler et al., 2013; USNRC, 2013; Bixler et al., 2020; Gauntt et al., 2003).

In the framework of thermal-hydraulics, great experience has been gained in performing uncertainty quantification analyses with thermal–hydraulic system codes, adopting the Best Estimate Plus Uncertainty approach (IAEA, 2008), and several international projects, such as the BEMUSE (Perez, 2011; OECD/NEA/CSNI, 2007; OECD/NEA/CSNI, 2011) and PREMIUM projects (OECD/NEA/CSNI, 2016; OECD/NEA/CSNI, 2017), have been conducted.

The HORIZON 2020 project "Management and Uncertainty of Severe Accident" (MUSA), led by CIEMAT (Spain) from 2019 to 2023, involved 28 organizations from 16 EU and non-EU countries and aimed to provide a harmonized approach for uncertainty and sensitivity analyses of SA sequences, moving beyond the state-of-the-art (Herranz et al., 2021; Herranz et al., 2025). The project regarded not only the modelling of SAs in Generation II and Generation III reactors, quantifying the codes uncertainties on selected Figures Of Merit (FOMs) related to ST, but also addressed SAs on spent fuel pools.

To achieve this purpose consistently and coherently, the project was divided into seven Working Packages (WPs). Among them, the WP "Application of UQ Methods against Integral Experiments" (AUQMIE) (Mascari, 2024), coordinated by ENEA (Italy), aimed to apply uncertainty methodologies and tools, developed by the partners of the project, against the internationally recognized Phebus FPT1 test. This test, conducted in the framework of the Phebus Programme (Jaquemain et al., 2000; Clément and Zeyen, 2013), represents a milestone for the state-of-the-art knowledge on cladding oxidation phenomena and fuel rod degradation during potential SA as well as Fission Products (FPs) chemistry and transport within the containment (Schwarz et al., 1999; de Luze et al., 2013; Kissane and Drosik, 2006; Simondi-Teisseire et al., 2013).

Considering that the FPT1 test represents a simplified but representative SA scenario, reproducing the in-vessel phase of a SA sequence in a Pressurized Water Reactor (PWR), the main target of the WP was to train the partners of the project to perform uncertainty quantification in the SA domain. The development of a code benchmark against experimental data was not the goal of the application: therefore, the experimental data provided by IRSN have been used for the calibration of the codes nodalization and to develop a proper reference case in view of the uncertainty application. The WP AUQMIE represented an important collaborative platform to highlight and discuss the results of uncertainty quantification analyses of the partners and the issues arising from the application of the methodologies and created a key technical background useful for the plant applications in Generation II and Generation III reactors and spent fuel pools giving a first contribution for the MUSA best practices and lessons learned. A more detailed summary of the WP AUQMIE is presented in (Mascari, 2024) and key insights and lessons learned on the uncertainty application against the Phebus FPT1 are presented in (Malicki and Lind, 2023; Elsalamouny and Kaliatka, 2021; Mascari et al., 2022; Tiborcz and Beck, 2024; Bocanegra and Herranz, 2022).

In the present activity, developed by ENEA along the WP AUQMIE, the uncertainty quantification analysis of the Phebus FPT1 has been conducted using the SA integral code MELCOR 2.2 (Humphries et al., 2023a,b) coupled with the Uncertainty Tool (UT) DAKOTA (Design Analysis Kit for Optimization and Terascale Application) (Dalbey et al., 2020; Adams et al., 2020). Several studies have been conducted using the MELCOR code to assess the Phebus FPT1 experiment concerning primary core degradation mechanisms (Wang et al., 2015) and material release from the bundle test (Darnowski et al., 2020). An uncertainty and sensitivity analysis on hydrogen generation in the Phebus FPT1 using the MELCOR 2.2 code is presented in (Darnowski et al., 2021).

The coupling between MELCOR and DAKOTA, presented in this work, has been developed in a Python environment/architecture adopting the probabilistic method to propagate input uncertainty (IAEA, 2008; Glaeser, 2008). The aim of the presented uncertainty application is to test the methodology estimating the uncertainties of the code on aerosol physics inside the containment. For this reason, the FOM selected for the study is the maximum value of the total mass of aerosol in suspension in the containment atmosphere of the facility. The uncertain input parameters selected for the uncertainty analysis are the aerosol miscellaneous constants. In the MELCOR code, these parameters are user-defined coefficients governing the aerosol dynamics, removal processes and particle interactions.

2. The Phebus program and the FPT1 test

Started in 1988 in France, the Phebus FP program involved five in-pile integral tests in view to investigate the degradation of nuclear fuel and the formation of pools of molten material, the production of hydrogen and the release of FPs from the fuel and their transport into the reactor coolant system. Furthermore, the test was focused on the deep study of aerosol physics and iodine chemistry (Schwarz et al., 1999; de Luze et al., 2013; Kissane and Drosik, 2006; Simondi-Teisseire et al., 2013).

The Phebus test fuel bundle replicated the core of a full-scale reactor and was made up of ten fuel rods, similar to those of a PWR, with an additional absorber rod of 1 m. An insulating zirconia shroud enveloped the test fuel bundle, which was placed inside an in-pile tube kept cooled by pressurized water.

The facility's experimental cooling circuit was composed of a hot leg, a cold leg, and a Steam Generator (SG) consisting of a single inverted U-tube. The containment of a full-scale PWR 900 MWe was simulated with a tank of about 10 m^3, considering a scale ratio of 5000:1. Condensed water was gathered into a sump and the steam was condensed by specific cooling structures.

Among the Phebus FP program experimental campaigns, the FPT1 examined the degradation of a bundle including two new fuel rods, eight irradiated fuel rods and a control rod made of silver, indium and cadmium. The test was composed of four main phases:

I. **Degradation Phase**: lasting about 5 h, this phase involved the degradation of the test fuel bundle. It was subdivided into two main parts: the thermal-calibration period, which endured about 7900 s, and a second part devoted to the temperature transient and bundle degradation. The latter was divided into pre-oxidation, oxidation, heat-up and cooling periods. During the pre-oxidation period, the test fuel bundle was heated, with initial cladding oxidation and hydrogen generation. The oxidation period was characterized by an initial ramp of bundle power and constant steam mass flow rate and, then, by a plateau of the bundle power, with the oxidation runaway and temperature escalation. After the plateau of the bundle power, at about 14,590 s after the start of the test, the heat-up period began. It was characterized by a second ramp of the bundle power, which causes the final heat-up of the fuel rods and the melting of the bundle material. At about 17,000 s the shutdown of the system was activated, and the cooling period began.

II. **Aerosol Phase**: it was devoted to the analysis of the airborne aerosols settled in the containment. It started about 18,000 s after the start of the test with the isolation of the containment.

III. **Washing Phase**: after about 64 h, the aerosols deposited on the containment floor were washed out into the sump water.

IV. **Chemistry Phase**: the temperature of the containment atmosphere was increased, and conditions were kept constant for about 18 h before the termination of the test to investigate the iodine chemistry in the sump.

3. The MELCOR code and the Phebus FPT1 nodalization

3.1. The MELCOR code

The fully integrated SA code MELCOR (Humphries et al., 2023a,b), developed by SNL for the USNRC, is capable of simulating transient thermal–hydraulic phenomena, as well as the main phenomena typical of a SA sequence involving the RPV, the reactor cavity and the containment with the estimation of the ST.

It is built upon a Control Volume (CV) modelling approach and features a modular structure characterized by different packages, each one simulating a different aspect of the transient phenomenology. Some of the MELCOR code packages used in the present activity are (Humphries et al., 2023b):

- *CAV package*: it models the attack of concrete by hot and molten core materials, computing the effect of heat transfer, concrete ablation, cavity shape change and gas generation.
- *COR package*: it performs calculations to determine the response of the reactor core and associated structures. It also evaluates the behavior of core debris in the Lower Plenum (LP) and its interaction with LP structures, including the lower head wall. It permits obtaining the transient response of these structures, modelling their relocation in the LP during an unmitigated transient sequence. Overall, the COR package simulates formation of debris, interaction of hot and degrading core with reactor structures, evaluation of the conditions under which failure of the lower head occurs leading to relocation of core debris into the reactor cavity.
- *CVH package and FL package*: they are responsible for modelling the thermal–hydraulic behaviour of coolant liquids and gases. They simulate the mass and energy transfer between CVs.
- *HS package*: it is responsible for calculating heat transfer between structures and the hydrodynamic material contained in the CVs. In general, a heat structure is defined as an intact solid structure, with one-dimensional thermal conduction heat transfer, with specific boundary conditions for each of the two surfaces. It can be characterized by a rectangular, cylindrical, spherical or hemispherical geometry.
- *RN package*: it models the behaviour of FPs, in the form of aerosols and vapours, as well as other trace species. Specific processes captured by the RN package include: radionuclide release from fuel and debris, aerosol dynamics with vapour condensation and re-vaporization, deposition on structure surfaces, transport through flow paths, and removal by engineered safety features.

Furthermore, the MELCOR code can be used through Symbolic Nuclear Analysis Package (SNAP), a state-of-the-art Graphic User Interface (GUI) for USNRC codes (Applied Programming Technology Inc., 2021). The MELCOR code version used for the application presented in this paper is MELCOR 2.2 18019.

3.2. The Phebus FPT1 nodalization

Starting from the input deck developed by USNRC (Humphries et al., 2015), the MELCOR nodalization of the Phebus FPT1 has been updated in SNAP to develop the reference case and, then, the uncertainty analysis.

A sketch of the MELCOR CVH package nodalization of the Phebus FPT1 is presented in Fig. 1. It is composed of 68 heat structures, 29 flow paths and 31 CVs. The rod bundle is axially divided into eleven CVs. Above the bundle, the vertical line is subdivided into the upper plenum, lower vertical line and upper vertical line. They have been modelled with three different CVs. Furthermore, two CVs are used to model the hot leg joining the vertical line and the SG inlet. Nine CVs on the ascending side and one on the descending side define the SG. The containment, modelled with a single CV, is connected to the SG outlet by two CVs. The fuel bundle test has been modelled with the MELCOR COR package with 31 axial and 2 radial regions to simulate core behaviour and degradation phenomena.

4. Reference case

The reference case has been developed considering the whole "degradation phase" simulating the thermal calibration period, pre-oxidation period, heat-up period and cooling period, described in Section 2. The beginning of the "aerosol phase" has been simulated not considering the subsequent iodine chemistry in the containment. The total simulation time is about 29,500 s. A total of six Phenomenological Windows (PhWs) have been identified (Table 1). They have been described concerning the phases of the experiment, described in Section 2.

The fission power and steam mass flow rate have been presented in Fig. 2. These data, provided along the WP AUQMIE of the MUSA project, have been implemented in the Phebus MELCOR input deck as boundary conditions.

The reference case has been analysed by considering the total mass of aerosol in suspension in the containment atmosphere. Other variables related to the thermal–hydraulic and bundle fuel behaviour (e.g. cladding temperature, containment pressure, etc.) are not part of this study, as they are the focus of other activities, performed with the same input deck and presented in (Humphries et al., 2015).

During the pre-oxidation phase of the test due to the linear increase of the power, the code predicts the start of the degradation of the fuel bundle and the release of iodine and caesium, leading to a small increase in the total mass of aerosol in suspension in the containment atmosphere. Fig. 3 compares the code prediction with the experimental data.

The subsequent oxidation phase is defined by a constant steam mass flow rate, a linear increase and then a plateau of the power. These conditions determine the runaway of cladding oxidation and the heat-up of the bundle, leading to the increase of release rate of FPs into the containment and, consequently, the increase of the total mass of aerosol in suspension in the containment atmosphere.

The linear rise of the power and the fall of steam mass flow rate drive the bundle test to the final degradation stage during the heat-up phase. At the end of this phase, at about 17,000 s after the start of the test, the total mass of aerosol in suspension in the containment atmosphere reaches the maximum value. In this regard, the code predicts a maximum value of about 59 g with a discrepancy of about 5 g from the experimental value, as shown in Fig. 3.

At about 17,000 s, following the system shutdown, a constant mass flow rate of steam is pumped into the bundle. Then, the isolation of the containment occurs about 18,600 s after the start of the test, initiating the aerosol phase characterized by the deposition of the aerosols into the inner containment surfaces (fallout).

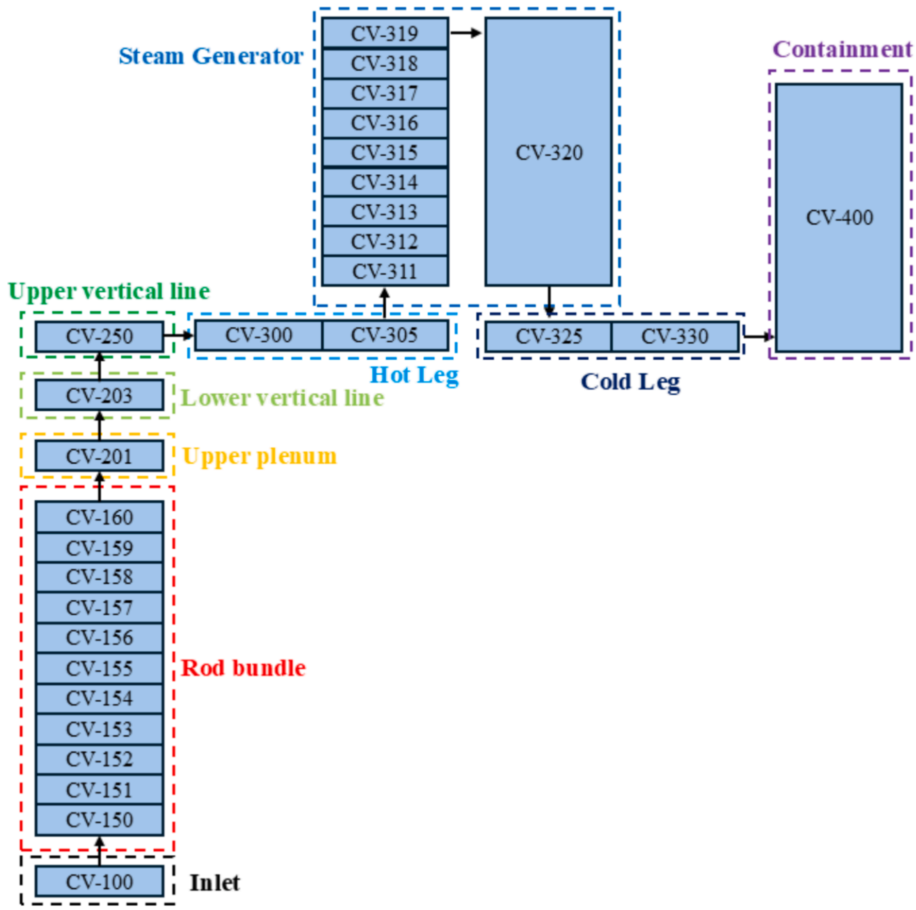

Fig. 1. Sketch of the CVH MELCOR nodalization of the Phebus FPT1.

Table 1
PhWs identified for the reference case.

N. [–]	Time [s]	Phenomenological Window	Experiment Phase
1	0–7900	Thermal-calibration period	Degradation Phase
2	7900–11060	Pre-oxidation period	
3	11060–14580	Oxidation period	
4	14580–17000	Heat-up period	
5	17000–18000	Cooling Period	
6	18000–29500	Beginning of the aerosol phase	Aerosol Phase

5. Uncertainty methodology

5.1. The probabilistic method

The present uncertainty application has been developed using the probabilistic method to propagate input uncertainty (IAEA, 2008; Glaeser, 2008): several different inputs are generated and run, each one characterized by different uncertain input values, which are sampled according to predefined Probability Density Function (PDF). Then, the uncertainty of the results is assessed by analysing the output FOMs.

A random Monte Carlo sampling of the PDFs of the selected uncertain input parameters is performed to obtain a number N of sets of parameters. The resulting N sets are used to develop N input decks that are successively run. To determine the minimum N, the Wilk's formula, presented in (Wilks, 1941; Wilks, 1942), can be used. It is based on the number of FOMs p and the desired probability content γ and confidence level β characterizing the FOMs. In this regard, more details on the statistical aspects can be found in (Guba et al., 2003).

In the present application, the study has been conducted considering the entire tolerance interval (two-sided tolerance interval). Then, the following Wilks' formula has been used to determine N (Guba et al., 2003):

$$\beta = 1 - \gamma^{N} - (N-1)(1-\gamma)\gamma^{N-1} \tag{1}$$

After the resolution on the N code runs, the statistical analysis of the code results is performed, with the evaluation of the main statistical parameters, such as the mean, median, maximum and minimum value, characterizing the FOM. Correlation coefficients such as the simple and simple rank coefficients can be computed to evaluate the statistical correlation between the FOMs and the selected uncertain input parameters (Gamble and Swiler, 2016; Rodgers and Nicewander, 1987).

5.2. The coupling of MELCOR and DAKOTA in a Python environment/architecture

DAKOTA (Dalbey et al., 2020; Adams et al., 2020) is an open-source software developed by SNL and designed to perform sensitivity analysis, optimization, parameter estimation, and parametric and uncertainty analyses in a fast and automatic way. DAKOTA can employ meta-algorithms to develop hybrid optimization, surrogate-based optimization, optimization under uncertainty or mixed aleatory/epistemic.

To develop an uncertainty analysis, DAKOTA is used at the beginning to sample the uncertain input parameters, characterized by their PDF and range of variation, through a selected sampling method to generate a set of N code inputs. After running the inputs, DAKOTA performs the statistical analysis of the extracted results and evaluates the main statistical variables of the FOMs. Furthermore, DAKOTA computes the correlation coefficients between the selected uncertain input parameters and the FOMs.

The study and the development of a computational environment for

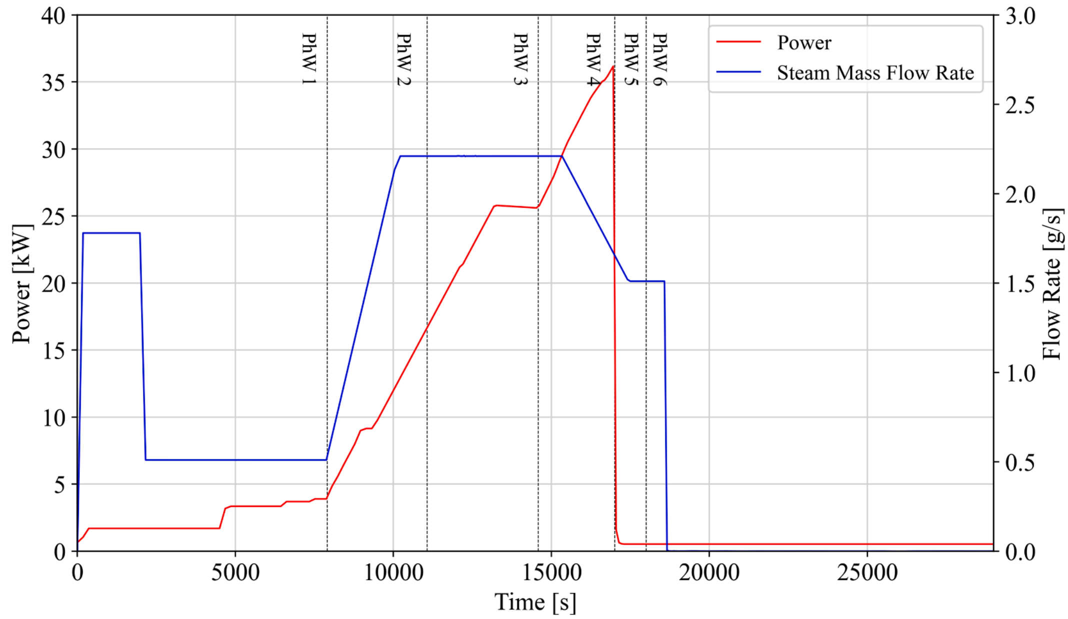

Fig. 2. Fission power and steam mass flow rate considered for the reference case.

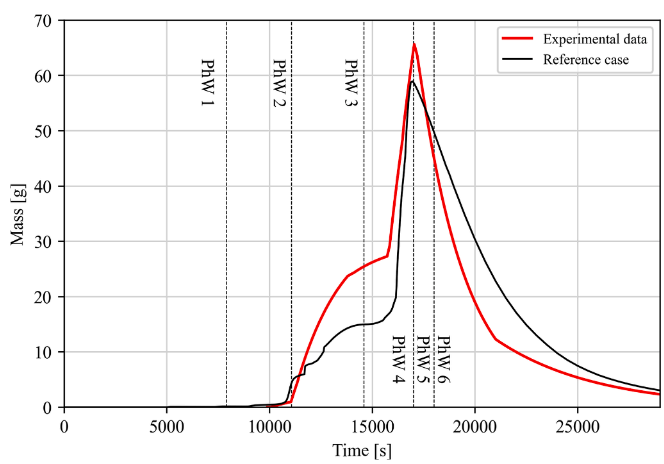

Fig. 3. Comparison of the total mass of aerosol in suspension in the containment atmosphere predicted by the code with the experimental data (Schwarz et al., 1999).

conducting uncertainty analysis with MELCOR code using DAKOTA started with the investigation of the coupling using SNAP described in (Mascari et al., 2024). To explore the capability of DAKOTA stand-alone, the coupling of MELCOR and DAKOTA in a Python environment has been developed by ENEA in collaboration with the University of Palermo in the framework of the WP AUQMIE of the MUSA project. The workflow of this coupling approach has been presented in Fig. 4.

The coupling is managed using the DAKOTA GUI and the main features of the uncertainty analysis are set through the DAKOTA input file. This latter is divided into three sections: Method, Interface and Responses. The Method section is related to the definition of the sampling method, the number of samples and characteristics of uncertain input parameters such as PDF type, mean value, upper and lower limits and standard deviation. This section permits to obtain *N* sets of uncertain input parameters, sampled by DAKOTA.

The Interface section manages the direct coupling between DAKOTA and MELCOR. The coupling is managed by a driver Python script. The driver script, first, substitutes, through an ad-hoc DAKOTA module called DPREPRO, the *N* sets of uncertain input parameters in the MELGEN and MELCOR template input decks, prepared in advance by the user, to create *N* sets of MELGEN and MELCOR input-decks. Then, the driver manages the MELCOR code runs and the extraction of the FOM channels from MELCOR calculation output files (which are.ptf type files) through the AptBatch executable (Applied Programming Technology, Inc., 2021). Concerning the possible failures of code runs, the driver script is set to ignore the failed code runs for the statistical analysis.

Finally, the Responses section is used to set the calculation of the statistics of the FOMs to be presented in the DAKOTA output file. An external in-house Python script has been developed to conduct the entire post-processing phase and the calculation of statistical parameters, profiting from the extensive post-processing capabilities offered by Python libraries. The external in-house Python script permits also to plot the dispersion plot of the extracted FOMs channels.

6. Uncertainty application

6.1. Hypotheses and uncertain input parameters description

The present application has the main objective of carrying out a full uncertainty analysis to test the methodology in the SA domain and to give some insights into the uncertainties of the MELCOR code related to aerosol physics. To achieve it, the maximum value of the total mass of aerosol in suspension in the containment atmosphere has been considered as FOM.

In MELCOR, aerosol phenomenology is based on the MAEROS code which is included in the RN package (Humphries et al., 2023b). Taking into account the phenomena occurring during a SA sequence, MAEROS simulates aerosol phenomenology such as condensation and evaporation of water and FPs to and from aerosol particles, particle agglomeration and deposition on surfaces, advection of aerosols between CVs and removal of aerosol particles by engineered safety features (Humphries et al., 2023a,b).

In MAEROS, some input parameters, called “aerosol miscellaneous constants” and selected by the user, permit the characterisation of aerosol dynamics and influence aerosol behaviour along MELCOR simulations.

The parameters influencing particle–particle interaction are:

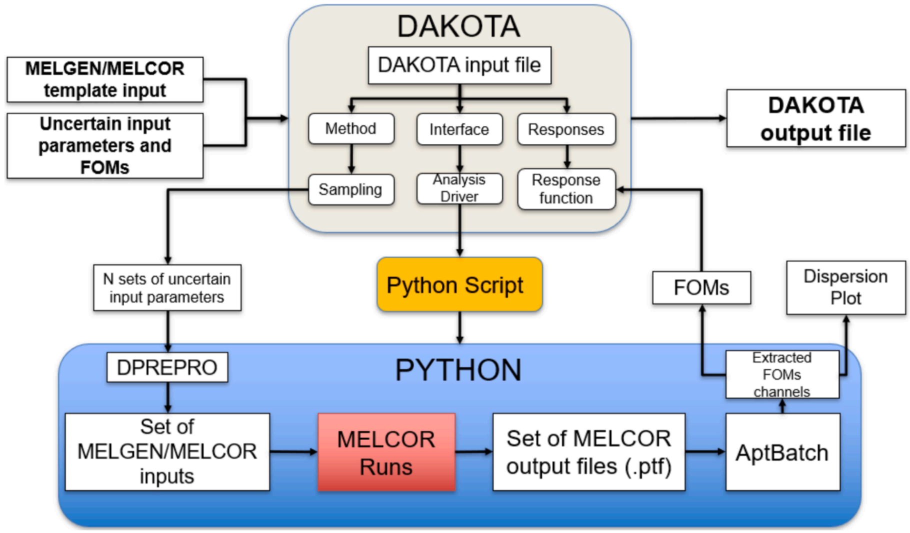

Fig. 4. Workflow of the coupling between MELCOR and DAKOTA in a Python environment/architecture.

- *Agglomeration shape factor*: it represents the effect of non-spherical shape upon aerosol collision cross sections. Unit values of the agglomeration shape factor correspond to a dense aerosol of spherical shape, while porous spherical agglomerates lead to values greater than unity (Humphries et al., 2023b).
- *Sticking coefficient*: it represents the agglomeration probability of two colliding particles (Herranz et al., 2013).
- *Turbolence energy dissipation density*: it considers the enhancement of agglomeration by turbulence in the atmosphere (Humphries et al., 2023b).

The parameters affecting the particle dynamics are:

- *Dynamic shape factor*: it represents the effect of non-spherical shape upon aerosol-atmosphere drag forces. Unit values of the dynamic shape factor correspond to dense aerosols of spherical shape, while porous spherical agglomerates lead to values greater than unity (Humphries et al., 2023b).
- *Particle slip coefficient*: it considers the momentum exchange between gas molecules and moving particles (Herranz et al., 2013).
- *Ratio of the gas-to-particle thermal conductivities*.

Finally, other parameters influence the aerosol removal processes:

- *Thermal accommodation coefficient*: fraction of thermal energy transferred from a particle to the surface on which it is depositing (Herranz et al., 2013).
- *Diffusion boundary layer thickness*: boundary layer for Brownian diffusion of aerosols. It determines the concentration gradient driving diffusion (Herranz et al., 2013).

These parameters have been chosen as uncertain input parameters for the following application. Table 2 shows the uncertain input parameters with their range of variation and PDF parameters (Humphries et al., 2023a,b; Humphries et al., 2015; Herranz et al., 2013; Gauntt et al., 2008).

To investigate the code uncertainty on the FOM, an approach based

Table 2
Uncertain input parameters selected for the present uncertainty application (Humphries et al., 2023a,b; Humphries, et al.2023; Herranz et al., 2013; Gauntt et al., 2008).

Parameter	Name in MELCOR	Unit	Reference value	Distribution type	Parameters	
Dynamic shape factor	**CHI**	[–]	1.0	Beta	β	1.5
					min	1.0
					max	5.0
Agglomeration shape factor	**GAMMA**	[–]	1.0	Beta	α	1.0
					β	1.5
					min	1.0
					max	5.0
Particle slip coefficient	**FSLIP**	[–]	1.257	Beta	α	4.0
					β	4.0
					min	1.2
					max	1.3
Sticking coefficient	**STICK**	[–]	1.0	Beta	α	2.5
					β	1.0
					min	0.5
					max	1.0
Turbolence dissipation rate	**TURBDS**	[m^2/s^3]	0.001	Uniform	min	0.00075
					max	0.00125
Ratio of the gas-to-particle thermal conductivities	**TKGOP**	[–]	0.05	Log-Uniform	min	0.006
					max	0.06
Thermal accommodation coefficient	**FTHERM**	[–]	2.25	Uniform	min	2.0
					max	2.5
Diffusion boundary layer	**DELDIF**	[m]	1.00E-05	Uniform	min	0.000005
					max	0.0002

on estimating the two-sided tolerance interval has been adopted, as previously introduced in section 5.1. According to equation (1), considering a probability and confidence level of 95 %, a minimum of 93 code runs are needed. In a conservative way before starting the uncertainty analysis, to consider possible failures of code runs, a total amount of 130 runs have been started following the strategy defined in (Mascari, 2024) related to the management of failed code runs. Considering this strategy of handling the failed code runs, they are not considered into account for the statistical analysis of the FOM but they are analyzed in the phase space of the normalized uncertain input parameters, as will be described in Section 6.2.

6.2. Results of the statistical analysis

The uncertainty analysis has been conducted on a single PC computation environment and a total of 10 failed code runs (less than 8 % of the total calculations) have been identified among the 130 total code runs. An approach based on the analysis of the phase space of the normalized (scaling considering the minimum and maximum for each parameter) parameters has been adopted. This approach permits an evaluation of the normalized uncertainty parameters values vs code failures. The visual observation of the results shows that the distribution of the failed code runs seems to be random and it is presented in Fig. 5.

The statistical analysis has been carried out through the calculation of the main statistical parameters of interest: the mean, the median, the lower and upper bounds, the standard deviation and the coefficient of variation. These are presented in Table 3.

Downstream of the propagation of the input uncertainties, the uncertainty band of the FOM is equal to 114.03 g, as presented in Table 3. The reference calculation value of 59 g, presented in Fig. 3, is within the uncertainty band calculated through the statistical analysis. In addition, the reference value is close to the mean and the median values, both of which are about 67 g, as shown in Table 3. After the running of the N code runs, the Cumulative Distribution Function (CDF) and PDF of the FOM have been calculated through the external Python script as well to characterize the code uncertainty. The calculated CDF and PDF are shown in Fig. 6 and Fig. 7 and they have been compared to the experimental value, the reference calculation, including the mean and median values, previously discussed. Furthermore, through Python, the FOM PDF kernel density estimation has been calculated to assess the shape of the theoretical PDF.

To characterize the uncertainty band of the code during all the simulated PhWs, the values of aerosol suspended mass in the containment atmosphere at each time-step have been compared to experimental values and the reference case along in the time domain. As presented in Fig. 8, the experimental data and the reference case are within the

Table 3
Statistical parameters of the FOM.

Statistical parameter	Unit	Value
Mean	[g]	67.14
Median	[g]	66.94
Lower bound	[g]	20.71
Upper bound	[g]	134.74
Uncertainty band	[g]	114.03
Standard deviation	[g]	25.60
Coefficient of variation	[–]	0.38

uncertainty band during all the simulated PhWs. As presented in this figure, the main statistical parameters have been computed at each time step of the calculation and compared with the experimental data. In this regard, a good agreement between the mean and the median value is found.

Fig. 9 shows the standard deviation associated with the uncertainty bandwidth at each time step and the coefficient of variation. The uncertainty bandwidth and, then, the standard deviation are equal to zero during PhW 1 and PhW 2. Then, due to the start of aerosol dynamics in the system, they increase during the oxidation period (PhW 3) and increase with a higher rate during PhW 4 (heat-up period), leading to the maximum value of the standard deviation of about 32 g during PhW 5, at around 16,000 s after the beginning of the test. This means that, in that part of the transient, the code results are affected by an uncertainty that can be characterized by the value of standard deviation and coefficient of variation. During PhW 3, PhW 4 and PhW 5 the coefficient of variation increases. Then, during the PhW 6, the uncertainty band and the standard deviation decreases and the coefficient of variation reaches a constant value of about 1.4 at the end of the simulated test.

6.3. Results of the statistical correlation analysis

The simple correlation coefficient and simple rank correlation coefficient have been calculated using, respectively, Pearson and Spearman's correlations. Based on the statistical correlation analysis, only the agglomeration shape factor shows a significant (negative) correlation. The other input uncertainty parameters have a low correlation with the FOM selected for analysis. The simple correlation coefficient, indicated with r, and the simple rank correlation coefficient, indicated as ρ, are reported in Fig. 10 and Fig. 11 for each uncertain input parameter.

The meaning of the correlation coefficients calculated above can be assessed through scatter plots, which represent the distribution and relationship between the FOM, and the value of a given uncertain input parameter. As a matter of example, in Fig. 12, the values of the FOM in the function of the values of the values of the agglomeration shape factor

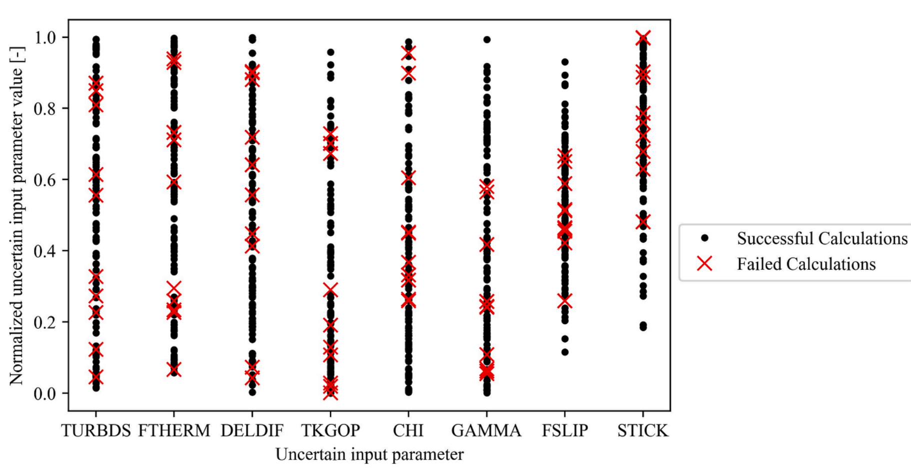

Fig. 5. Normalized uncertain input parameters phase space.

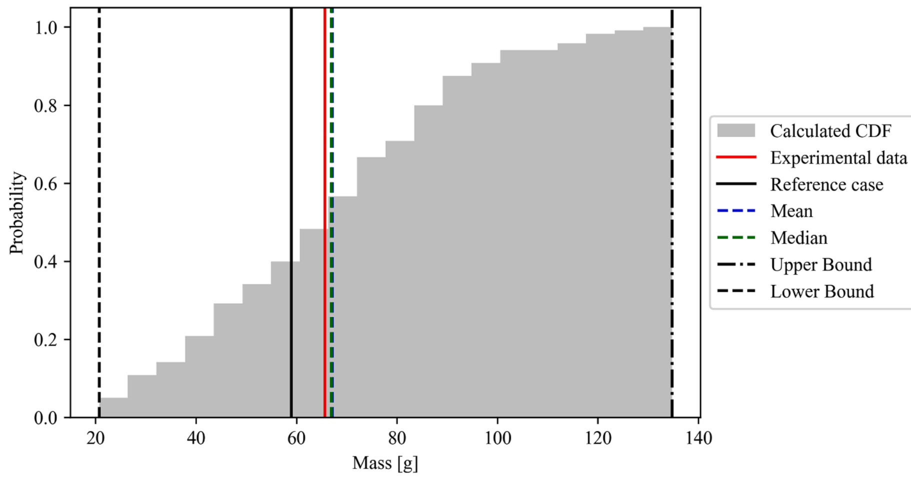

Fig. 6. Calculated CDF of the FOM (Schwarz et al., 1999).

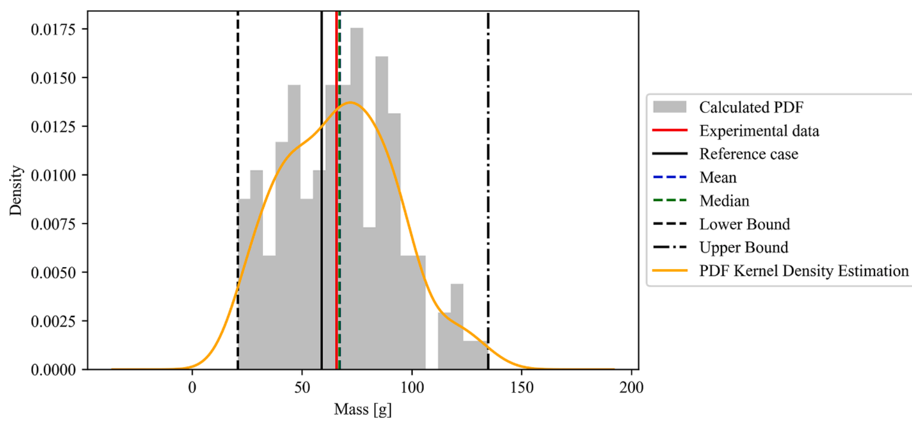

Fig. 7. Calculated PDF of the FOM (Schwarz et al., 1999).

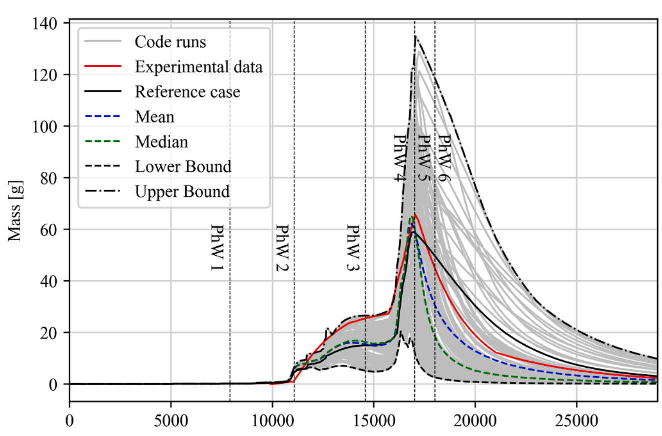

Fig. 8. Uncertainty band of the total mass of aerosol in suspension in the containment atmosphere during the simulated experiment (Schwarz et al., 1999).

have been represented. The statistical correlation has been also highlighted using the linear regression technique and the calculation of a trend curve.

The simple and simple rank correlation coefficients have been also calculated starting from the beginning of the oxidation period since the uncertainty band before that time is absent. They have been shown in

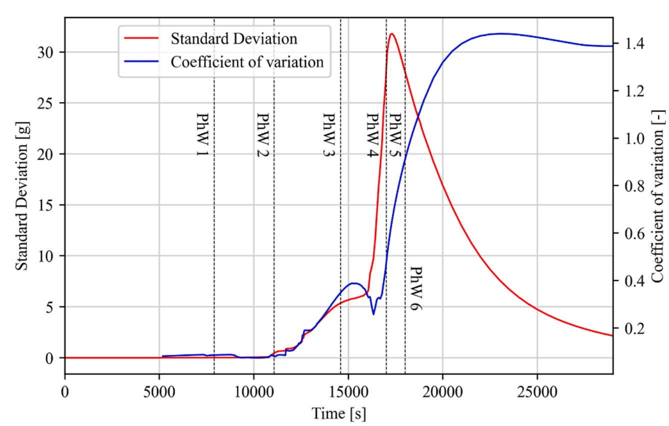

Fig. 9. Standard deviation and coefficient of variation.

Fig. 13 and Fig. 14.

The dynamic shape factor is positively correlated with the total aerosol mass in the containment atmosphere until the middle of the PhW 3. This part of the transient is characterized by the release of FPs in the form of aerosol from the test bundle to the containment. Increasing values of the dynamic shape factor determine aerosol particles with a greater tendency to diverge from particles with spherical shape (as discussed in Section 6.1) and thus with a greater aerosol-atmosphere drag force. It implies a greater tendency for particles to stay in the

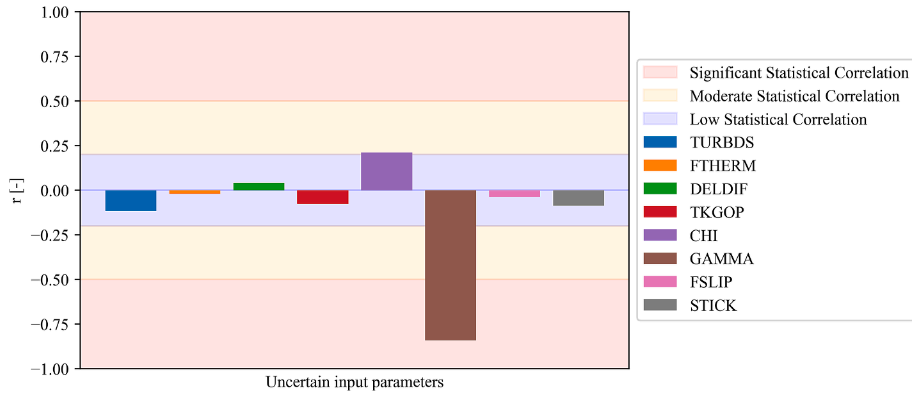

Fig. 10. Simple correlation coefficient.

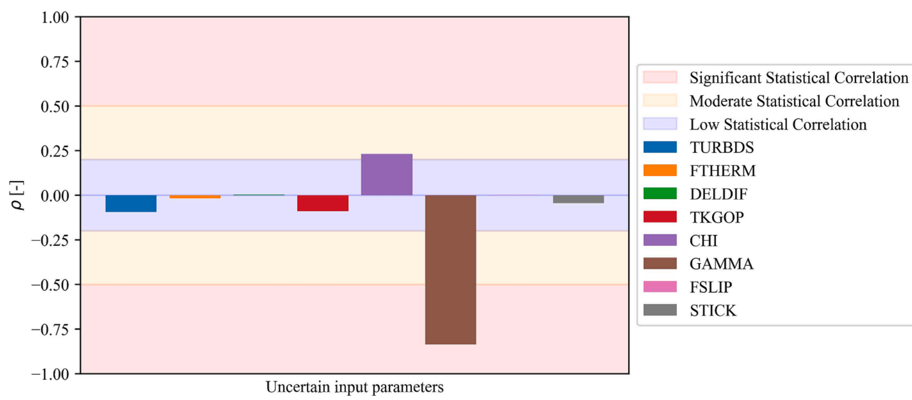

Fig. 11. Simple rank correlation coefficient.

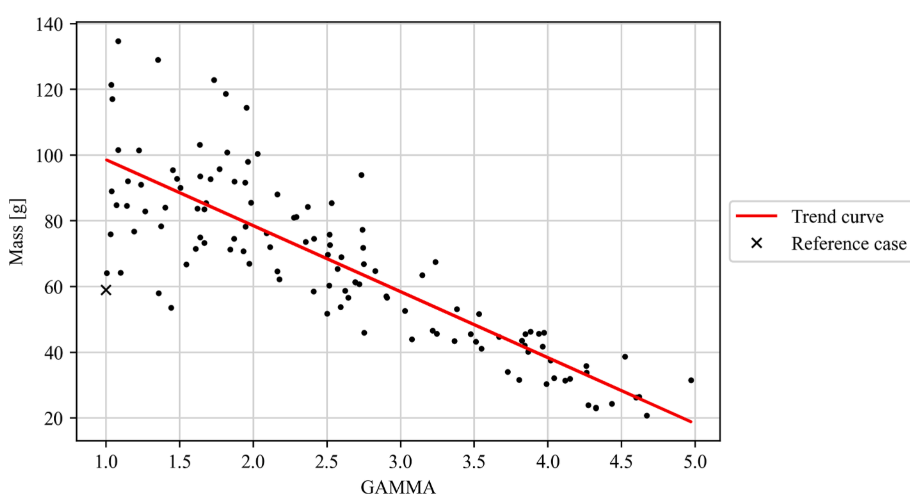

Fig. 12. Scatter plot of the FOM and values of the agglomeration shape factor.

containment atmosphere and thus an increase in the total mass of aerosol in the containment atmosphere. In the second half of PhW 3, the statistical correlation between the total mass of aerosol in the containment atmosphere and the dynamic shape factor parameter decreases from significant to moderate, suggesting that, at this stage, this effect reduces its intensity on the content of aerosol mass in the containment atmosphere.

After the second half of PhW 3, considering the increased amount of aerosol particles in the containment atmosphere, the agglomeration forces become preponderant. For this reason, the statistical correlation between the agglomeration shape factor and the total mass of aerosol in the containment atmosphere changes from low to moderate, and finally, significant. This means that an increase in the agglomeration shape factor corresponds to a greater tendency for aerosol particles to agglomerate and settle on the containment surfaces. The net effect of this phenomenon is the reduction in the total mass of aerosols in the containment atmosphere and, for this reason, the statistical correlation turns out to be negative. All other uncertain input parameters present a low statistical correlation throughout the whole simulation.

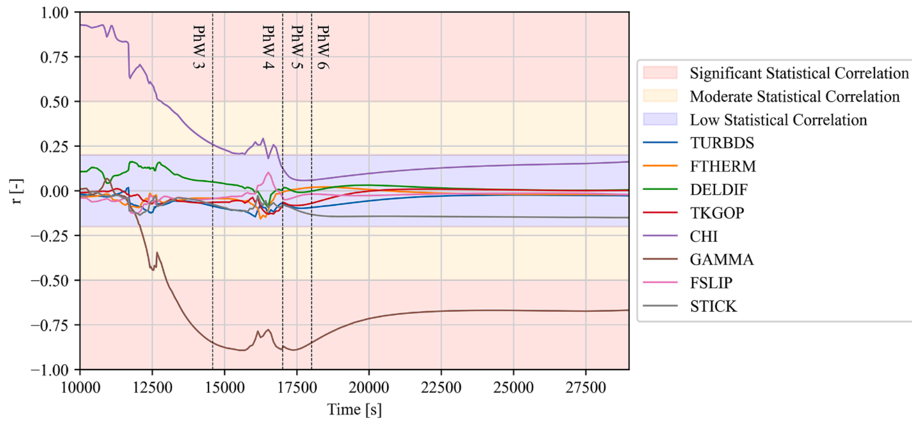

Fig. 13. Simple correlation coefficient along the simulated phases.

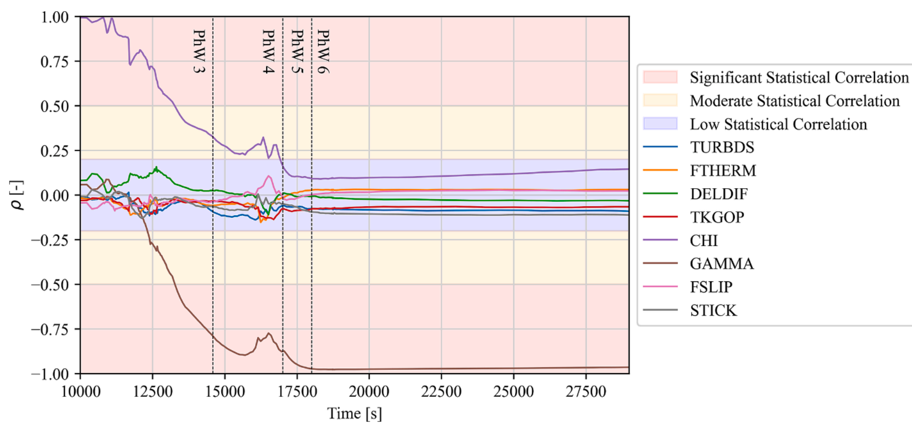

Fig. 14. Simple rank correlation coefficient along the simulated phases.

7. Conclusions

In the last few years, the international nuclear scientific community has focused its interest on the development of uncertainty quantification methodology in the field of SA. The methodologies, well established for the development of uncertainty analyses for thermal–hydraulic codes, have been reviewed and applied in the framework of the EU-MUSA project, which aims to establish a harmonized approach, among both EU and non-EU entities, for the analysis of uncertainties and sensitivities associated with SAs.

In the present activity, performed by ENEA in the framework of the WP AUQMIE of the MUSA project, the uncertainty quantification analysis against the internationally recognized Phebus FPT1 has been developed. The reference case, conducted with the SA integral code MELCOR, has been developed by analyzing the total mass of aerosol in suspension in the containment atmosphere considering the degradation phase and the beginning of the aerosol phase of the test.

To conduct the uncertainty analysis, the coupling of MELCOR and DAKOTA in a Python environment/architecture, developed by ENEA in collaboration with the University of Palermo, has been adopted. This coupling framework allows conducting an uncertainty application using the capabilities of DAKOTA.

In this study, the statistical analysis of the results has been developed by using an in-house Python script which performs the full post-processing of the results (e.g. plot of the results, export of the spreadsheet, etc.) as well. The aerosol miscellaneous constants, defined by the user in MELCOR, have been considered as uncertain input parameters and the maximum value of the total mass of aerosol in suspension in the containment atmosphere as FOM of the uncertainty analysis.

To conduct the uncertainty analysis, the probabilistic method to propagate input uncertainty has been considered. Based on Wilks' method, the minimum number of calculations N, considering the two-sided tolerance interval, to obtain a probability and confidence level of 95 %, is 93 but, accounting for potential code run failures, a total of 130 code runs have been considered. A total of 10 failed runs (less than 8 % of the total code runs) have been encountered during the analysis and have been discarded. Through the analysis of the phase space of the sampled uncertain input parameters, the failure of these runs seems to be random.

The statistical analysis has been conducted by computing the empirical CDF and PDF of the FOM and the main statistical parameters such as mean, median, standard deviation, coefficient of variation, and upper and lower bound. The analysis of the uncertainty band of code results shows that both the experimental data and the reference case lie within the evaluated uncertainty band. The statistical correlation analysis, with the simple and simple rank coefficients for each uncertain input parameter, highlights a linear and monotonous significant negative correlation of the agglomeration shape factor with the FOM.

To gain insights into the code uncertainties along the simulated test, the total mass of aerosol in suspension in the containment atmosphere at each run and at each time-step has been compared with the reference case, experimental data and the main statistical parameters such as mean, median, upper and lower bound. The standard deviation and the coefficient of variation have been computed at each time step as well. The uncertainty band is small along the thermal calibration phase and begins to increase with the pre-oxidation phase, reaching its maximum width about 16,000 s after the start of the test. The statistical correlation analysis has been performed during the simulated transient as well, with the evaluation of the simple and simple rank coefficients, showing a linear and monotonous correlation of the FOM with the dynamic shape factor and agglomeration shape factor, with different significance depending on the test phase.

The present work permitted to setting up of a complete uncertainty quantification analysis in the SA domain testing the computational framework and the methodology. It permitted to have fundamental insights into the MUSA project, preparing the partners for the plant application described in Brumm (2025).

CRediT authorship contribution statement

Giuseppe Agnello: Writing – review & editing, Writing – original draft, Visualization, Software, Methodology, Conceptualization. **Mattia Massone:** Writing – review & editing, Writing – original draft, Software, Investigation. **Fulvio Mascari:** Writing – review & editing, Writing – original draft, Supervision, Resources, Methodology, Investigation, Conceptualization.

Declaration of competing interest

The authors declare that they have no known competing financial interests or personal relationships that could have appeared to influence the work reported in this paper.

Acknowledgements

This project has received funding from the Euratom research and training programme 2014-2018 under grant agreement No 847441. This paper reflects only the author's view, and the European Commission is not responsible for any use that may be made of the information it contains.

ENEA carried out the research activity with MELCOR code and SNAP, obtained in the framework of the ENEA-ISIN agreement signed on March 23rd 2020 as part of the General Arrangement between the United States Nuclear Regulatory Commission (US-NRC) and the Italian National Inspectorate for Nuclear Safety and Radiation Protection (ISIN).

The authors gratefully acknowledge USNRC and SNL for their valuable comments and suggestions during the preparation of the manuscript.

Data availability

Data will be made available on request.

References

Adams, B.M., Bohnhoff, W.J., Dalbey, K.R., Ebeida, M.S., Eddy, J.P., Eldred, M.S., Hooper, R.W., Hough, P.D., Hu, K.T., Jakeman, J.D., Khalil, M., Maupin, K.A., Monschke, J.A., Ridgway, E.M., Rushdi, A.A., Seidl, D.T., Stephens, J.A., Swiler, L.P., Winokur, J.G., Dakota, 2020. A Multilevel Parallel Object-Oriented Framework for Design Optimization, Parameters Estimation, Uncertainty Quantification, and Sensitivity Analysis: Version 6.13 User's Manual.

Applied Programming Technology Inc., 2021. Symbolic Nuclear Analysis Package (SNAP) User's Manual.

Applied Programming Technology, Inc., 2021. *AptPlot User's Manual*.

Bixler, N.E., Dennis, M., Ross, K., Osborn, D.M., Gauntt, R.O., Wagner, K.C., Ghosh, S.T., Hathaway, A.G., Esmaili, H., 2020. SOARCA uncertainty analysis of a short-term station blackout accident at the Sequoyah nuclear power plant. *Ann. Nucl. Energy* 145 (107495).

Bixler, N., Gauntt, R., Jones, J., Leonard, M., 2013. State-of-the-Art Reactor Consequence Analyses Project, Volume 1: Peach Bottom Integrated Analysis, NUREG/CR-1710, Albuquerque, New Mexico.

Bocanegra, R., Herranz, L.E., 2022. CIEMAT's outcomes from the PHEBUS-FPT1 uncertainty analysis in the framework of the EU-MUSA project, in The 10th European Review Meeting on Severe Accident Research (ERMSAR2022), Karlsruhe, Germany, May 16-19.

Brumm, S., et al., 2025. Uncertainty quantification for severe-accident reactor modelling: Results and conclusions of the MUSA reactor applications work package. *Ann. Nucl. Energy* 211 (110962).

Chatelard, P., Belon, S., Bosland, L., Carénini, L., Coindreau, O., Cousin, F., Marchetto, C., Nowack, H., Piar, L., Chalain, L., 2016. Main modelling features of the ASTEC V2.1 major version. *Ann. Nucl. Energy* 93, 83–93.

Clément, B., Zeyen, R., 2013. The objectives of the Phebus FP experimental programme and main findings. *Ann. Nucl. Energy* 61, 4–10.

Dalbey, K.R., Eldred, M.S., Geraci, G., Jakeman, J.D., Maupin, K.A., Monschke, J.A., Seidl, D.T., Swiler, L.P., Tran, A., Menhorn, F., Zeng, X., Dakota, 2020. A Multilevel Parallel Object-Oriented Framework for Design Optimization, Parameter Estimation, Uncertainty Quantification, and Sensitivity Analysis: Version 6.13 Theory Manual.

Darnowski, P., Włostowski, M., Stepien, M., Niewinski, G., 2020. Study of the material release during PHEBUS FPT-1 bundle phase with MELCOR 2.2. *Ann. Nucl. Energy* 148 (107700).

Darnowski, P., Mazgaj, P., Włostowski, M., 2021. Uncertainty and Sensitivity Analysis of the In-Vessel Hydrogen Generation for Gen-III PWR and Phebus FPT-1 with MELCOR 2.2. Energies 14 (4884).

de Luze, O., Haste, T., Barrachin, M., Repetto, G., 2013. Early phase fuel degradation in Phébus FP: Initiating phenomena of degradation in fuel bundle tests. *Ann. Nucl. Energy* 61, 23–35.

Elsalamouny, N., Kaliatka, T., 2021. Uncertainty quantification of the PHEBUS FPT-1 test modelling results. Energies 4 (7320).

EPRI, 2016. Modular Accident Analysis Program Version 5.04, EPRI Product ID 3002007340, Vol. 1-4.

Gamble, K.A., Swiler, L.P., 2016. Uncertainty Quantification and Sensitivity Analysis Applications to Fuel Performance Modeling, SAND2016-4597C.

Gauntt, R.O., Bixler, N.E., Wagner, K., 2003. An Uncertainty Analysis of the Hydrogen Source Term for a Station Blackout Accident in Sequoyah Using MELCOR 1.8.5, SAND2014-2210. Albuquerque, New Mexico.

Gauntt, R.O., Radel, T., Salay, M.A., Kalinich, D.A., 2008. Analysis of Main Steam Isolation Valve Leakage in Design Basis Accidents Using MELCOR 1.8.6 and RADTRAD, SAND2088-6601, 2008.

Glaeser, H., 2008. GRS method for uncertainty and sensitivity evaluation of code results and applications. *Sci. Technol. Nucl. Install.* 798901, 2008.

Guba, A., Makai, M., Pal, L., 2003. Statistical aspects of best estimate method-I. *Reliab. Eng. Syst. Saf.* 80, 217–232.

Herranz, L.H., Beck, S., Sánchez-Espinoza, V.H., Mascari, F., Brumm, S., Coindreau, O., Paci, S., 2021. The EC MUSA project on management and uncertainty of severe accidents: main pillars and status. Energies 14 (4473).

Herranz, L.E., Garcia, M., Morandi, S., 2013. Benchmarking LWR codes capability to model radionuclide deposition within SFR containments: An analysis of the Na ABCOVE tests. *Nucl. Eng. Des.* 265, 772–784.

Herranz, L.E., Beck, S., Sànchez-Espinoza, V.H., Mascari, F., Brumm, S., Coindreau, O., Paci, S., 2025. Major Achievements of the EC MUSA Project. Nucl. Technol. 1–11.

Humphries, L.L., Louie, L., Figueroa, V., Young, M., Weber, S., Ross, K., Phillips, J., Jun, R., 2015. MELCOR Computer Code Manuals Vol.3: MELCOR Assessment Problems Version 2.1.7347, SAND 2015-6693 R, Albuquerque (USA).

Humphries, L.L., Beeny, B.A., Gelbard, F., Haskin, T., Louie, D., Phillips, J., Reynolds, J., C. Schimidt, R.C., 2023. MELCOR Computer Code Manuals: Vol. 2: Reference Manual Version 2.2 r2023.0, Sandia National Laboratories, Albuquerque (USA).

Humphries, L.L., Beeny, B.A., Gelbard, F., Haskin, T., Phillips, J., Reynolds, J., Schmidt, R.C., 2023. MELCOR Computer Code Manuals: Vol. 1: Primer and User's Guide Version 2.2 r2023.0, Sandia National Laboratories, Albuquerque (USA).

IAEA, 2008. Safety Reports Series No.52: Best Estimate Safety Analysis for Nuclear Power Plants. Uncertainty Evaluation, Vienna.

Jaquemain, D., Bourdon, S., de Braemaeker, A., Barrachin, M., 2000. PHEBUS FPT1 Final Report, IPSN/DRS/SEA/PEPF Report SEA1/00,IP/00/479. Cadarache, France.

Kissane, M.P., Drosik, I., 2006. Interpretation of fission-product transport behavior in the Phebus FPT0 and FPT1 tests. *Nucl. Eng. Des.* 236, 1210–1223.

Malicki, M., Lind, T., 2023. Parametric MELCOR 2.2 sensitivity and uncertainty study with a focus on aerosols based on Phébus test FPT1. Prog. Nucl. Energy 158 (104609).

Mascari, F., et al., 2024. Main outcomes of the Phebus FPT1 uncertainty and sensitivity analysis in the EU-MUSA project. *Ann. Nucl. Energy* 196 (110205).

Mascari, F., Nakamura, H., Umminger, K., De Rosa, F., D'Auria, F., 2015. Scaling issues for the experimental characterization of reactor coolant system in integral test facilities and role of system code as extrapolation tool, Vol. %1 di %2NURETH-16, August 30–September 4.

Mascari, F., Massone, M., Agnello, G., Angelucci, M., Paci, S., D'Onorio, M., Giannetti, F.. 2022. PHEBUS FPT1 uncertainty application with the melcor 2.2 CODE, in 19th International Topical Meeting on Nuclear Reactor Thermal Hydraulics (NURETH19), Brussels, Belgium, March 6 - 11, 2022.

Mascari, F., Rocchi, F., Carny, P., Liptak, L., Adorni, M., Fontanet, J., Herranz, L.E., 2019. FASTNET SCENARIOS DATABASE DEVELOPMENT AND STATUS. The 9th European Review Meeting on Severe Accident Research (ERMSAR2019), Prague, Czech Republic, March 18-20.

Mascari, F., De La Rosa Blul, J.C., Sangiorgi, M., Bandini, G., 2019. Analyses of an Unmitigated Station Blackout Transient in a Generic PWR-900 with ASTEC, MAAP and MELCOR Codes. NUREG/IA-0515.

Mascari, F., Bersano, A., Agnello, G., Angelucci, M., Phillips, J., Luxat, D., 2024. MELCOR - DAKOTA coupling for uncertainty analyses in the SNAP environment/architecture. *Nucl. Eng. Des.* 421 (113078).

NEA/CSNI, 2001. In-Vessel Core Degradation Code Validation Matrix Update 1996-1999, NEA/CSNI/R(2000)21.

NEA/CSNI, 2024. Containment Code Validation Matrix, NEA/CSNI/R(2014)3.

OECD/NEA/CSNI, 1992. Source term uncertainty, recent development in understanding fission product behavior, NEA/CSNI/R(92)2.
OECD/NEA/CSNI, 1996. SOAR on Containment Thermalhydraulics and Hydrogen Distribution, NEA/CSNI/R(1999)16.
OECD/NEA/CSNI, 2007. BEMUSE Phase III Report: Uncertainty and Sensitivity Analysis of the LOFT L2-5 Test, NEA/CSNI/R(2007)4.
OECD/NEA/CSNI, 2009. State-Of-The-Art Report On Nuclear Aerosols, NEA/CSNI/R (2009), 2009.
OECD/NEA/CSNI, 2011. BEMUSE Phase VI Report: Status Report on the Area, Classification of the Methods. Conclusion and Recommendations, NEA/CSNI/R (2011)4.
OECD/NEA/CSNI, 2016. PREMIUM: A Benchmark on the Quantification of the Uncertainty of the Physical Models in the System Thermal-hydraulic Codes. Methodologies and Data Review, NEA/CSNI/R(2016)9.
OECD/NEA/CSNI, 2017. Post-BEMUSE Reflood Model Input Uncertainty Methods (PREMIUM) Benchmark - Final Report, NEA/CSNI/R(2016)18.
Perez, M., et al., 2011. Uncertainty and sensitivity analysis of a LBLOCA in a PWR Nuclear Power Plant: Results of the Phase V of the BEMUSE programme. *Nucl. Eng. Des.* 241, 4206–4222.
Rodgers, J.L., Nicewander, A., 1987. Thirteen Ways to Look at the Correlation Coefficient. *Am. Stat.* 42, 59–66.
Schwarz, M., Hache, G., von der Hardt, P., 1999. PHEBUS FP: a severe accident research programme for current and advanced light water reactors. *Nucl. Eng. Des.* 187, 47–69.
Simondi-Teisseire, B., Girault, N., Payot, F., Clément, B., 2013. Iodine behavior in the containment in Phébus FP tests. *Ann. Nucl. Energy* 61, 157–169.
Tiborcz, L., Beck, S., 2024. Uncertainty and sensitivity analysis of the fission product behaviour in the Phébus FPT1 test with the system code AC2. *Nucl. Eng. Des.* 429 (113594).
USNRC, 2013. State-of-the-Art Reactor Consequence Analyses Project, Volume 2: Surry Integrated Analysis, NUREG/CR-7110, Albuquerque, New Mexico.
Van Dorsselaere, J.P., Mustoe, J., Power, S., Adorni, M., Schaffrath, A., Nieminen, A., 2016. ETSON views on R&D priorities for implementation of the 2014 Euratom Directive on safety of nuclear installations. *Kerntechnik* 81 (5), 527–534.
Wang, J., Corradini, M.L., Fu, W., Haskin, T., Zhang, Y., Tian, W., Su, G., Qiu, S., 2015. Simulation of the PHEBUS FPT-1 experiment using MELCOR and exploration of the primary core degradation mechanism. *Ann. Nucl. Energy* 85, 193–204.
Wilks, S.S., 1941. Determination of sample size for setting tolerance limits. *Ann. Math. Stat.* 12, 91–96.
Wilks, S.S., 1942. Statistical prediction with special reference to the problem of tolerance limits. *Ann. Math. Stat.* 13, 400–409.